SAFEST V1.1 Antenna Datasheet

Introduction

SAFEST V1.1 (FCC ID: 2BEKJ-SAFESTV1-1) is a human activity monitor that leverages a Texas Instruments 64GHz mmWave radar chip with 7 antennas on package (IWR6843AOP, 3 transmitter and 4 receiver antennas).

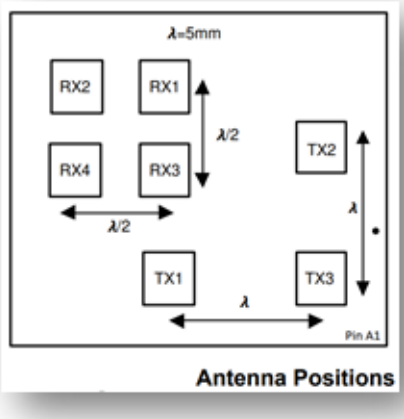

SAFEST V1.1 also utilizes an Espressif Systems ESP32 microprocessor which has embedded Wi-FI, Bluetooth Classic, Bluetooth LE, and 2 antennas on package (ESP32-WROOM-DA-N16, FCC ID: 2AC7Z-ESPWROOMDA). This diagram shows these 2 antennas (ANT1 and ANT2) and their distance to IWR6843AOP's closest transmitter, TX2 (33mm):

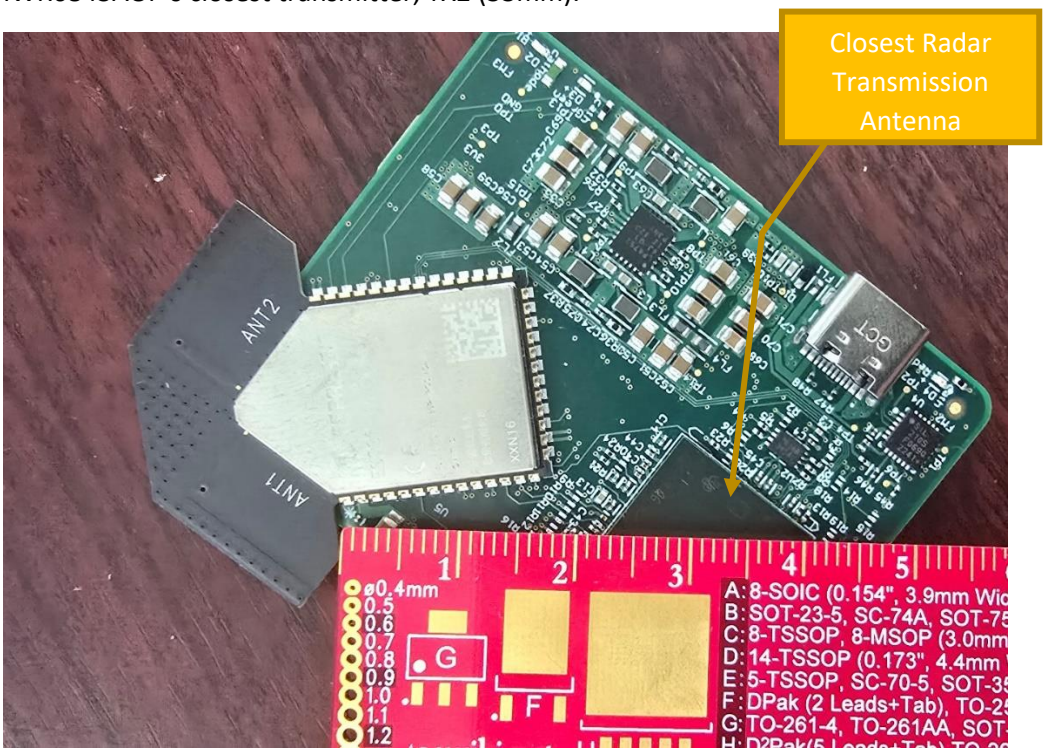

IWR6843AOP mmWave Radar Antenna Gain

The IWR6843AOP antenna gain was obtained from the manufacturer's website (https://www.ti.com/lit/an/swra705/swra705.pdf Pages 11 and 14. Entire document is incorporated at the end of this Antenna Datasheet). The typical gain for the IWR6843AOP in the direction of maximal radiation is 7.74dB:

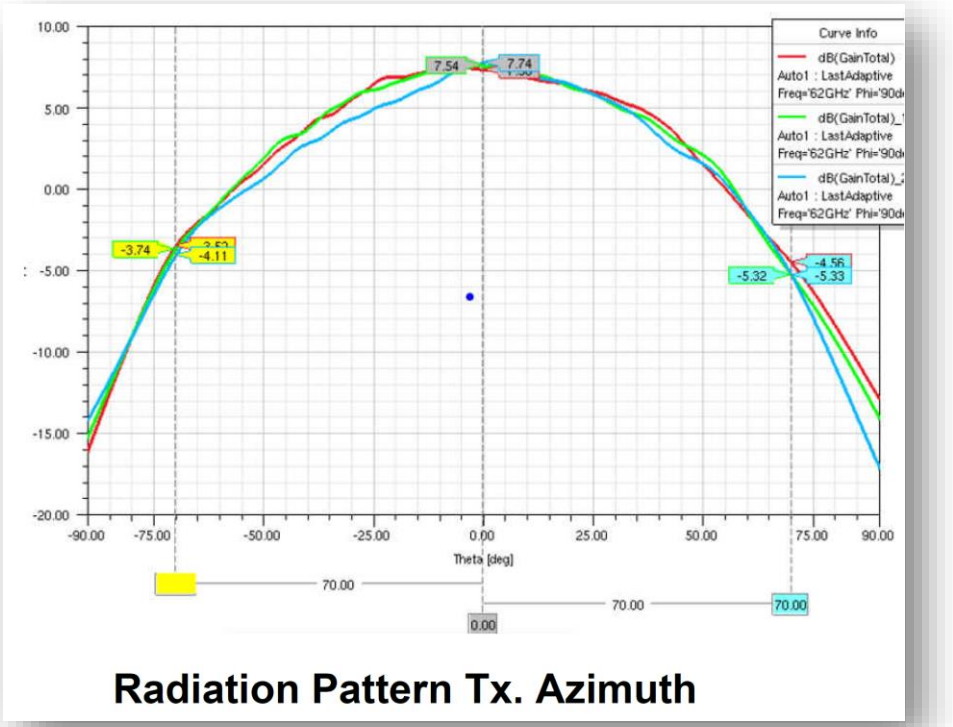

Radiation Pattern Tx. Azimuth

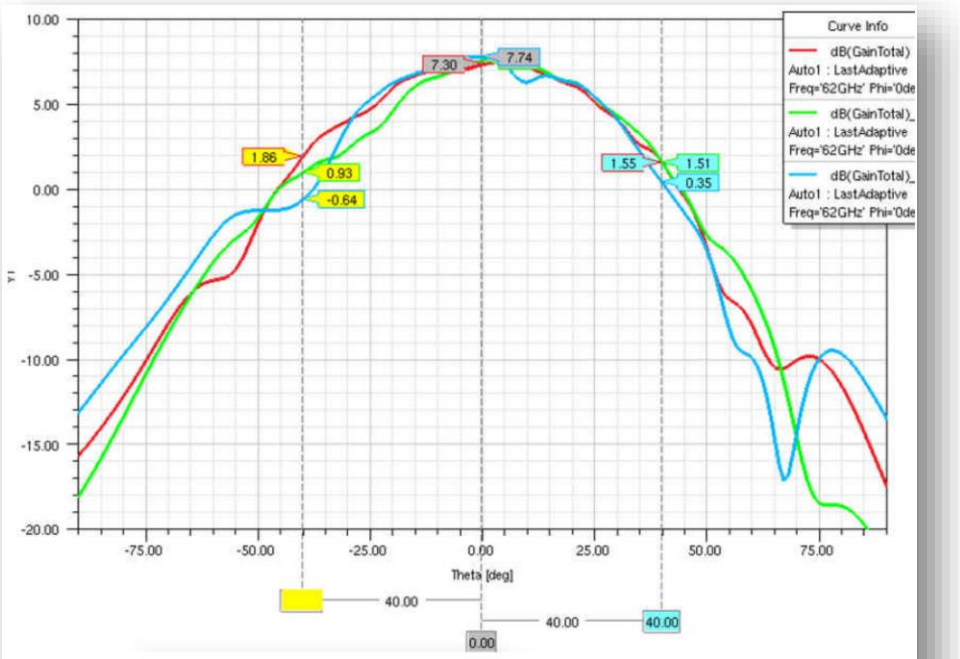

Radiation Pattern Tx. Elevation

The output is fairly consistent across all frequencies utilized as obtained from the manufacturer's website (https://www.ti.com/lit/ds/symlink/iwr6843aop.pdf Page 34):

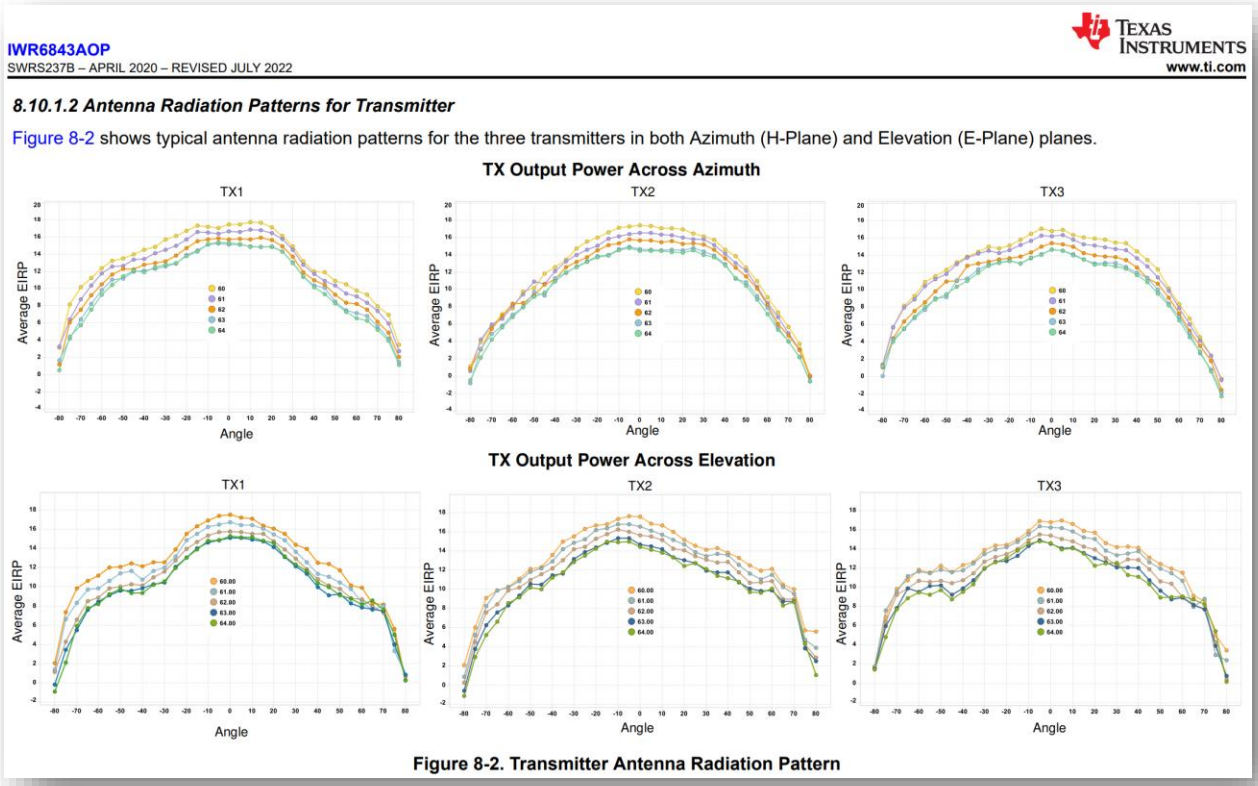

Figure 8-2. Transmitter Antenna Radiation Pattern

Given that the IWR6843AOP radar chip in SAFEST uses a frequency band greater than 500MHz but less than 4GHz, SAFEST meets the FCC requirement which limits peak radiated power to +10 dBm and peak conducted power to -10 dBm.

In order to accomplish this, SAFEST V1.1 is configured to attenuate the transmission power. As configured, SAFEST V1.1's measured IWR6843AOP's maximum EIRP ($P_{radiated}$) = -3.77dBm = $P_{conducted}$ + $G_{antenna}$:

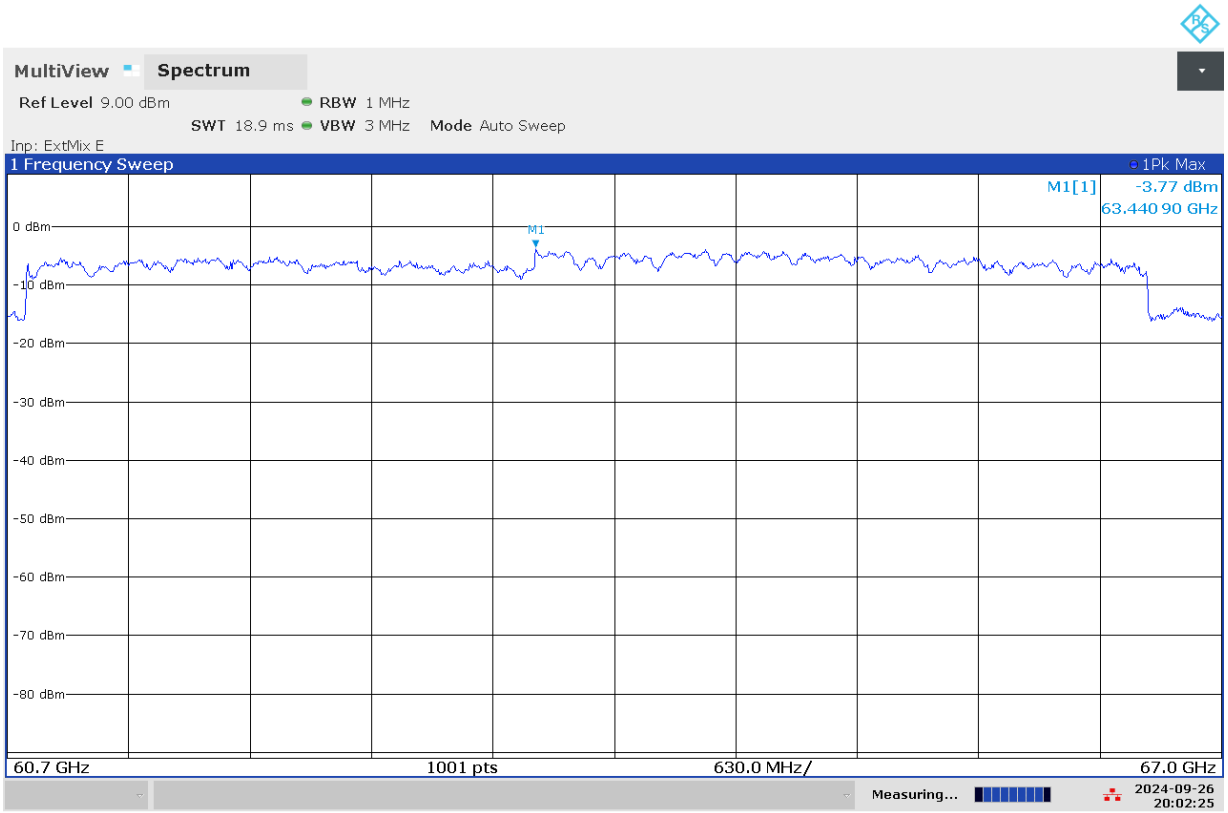

08:02:25 PM 09/26/2024

Note 1: Hand scans were performed at close distance around the EUT with vertical and horizontal polarities to find the maximum emissions. The antenna was then moved and placed in a far field at 0.52 m.

Note 2: All factors, mixer conversion loss, antenna factors, cable factors, path loss factors, and distance factors were internally compensated.

Product Standard: CFR47 FCC Part 15.255				Limit applied: 10 dB(m) Pretest Verification w/BB source: Yes			
Test Date	Test Personnel/ Initials	Supervising Engineer/ Initials	Input Voltage	Mode	Atmospheric Data		
					Temp C°	Relative Humidity %	Atmospheric Pressure mbar
09/26/2024	Vathana Ven	N/A	120VAC 60Hz	Continuous sweep	24	48	1010

Deviations, Additions, or Exclusions: None

Given that the typical maximum $G_{antenna}$ for the IWR6843AOP is 7.74dB, the SAFEST V1.1 $P_{conducted}$ = -3.77dBm - 7.74dB = -11.51dBm which is below the -10dBm limit.

ESP32-WROOM-DA-N16 Antenna Gain

The ESP32-WROOM-DA-N16 is an ESP32 microprocessor which has embedded Wi-FI, Bluetooth, Bluetooth LE, and 2 antennas on package (FCC ID: 2AC7Z-ESPWROOMDA). Its antenna gain was obtained from the manufacturer's FCC RF Exposure Report (https://fcc.report/FCC-ID/2AC7Z-ESPWROOMDA/5597064 RF_Exposure_Report Page 11) and was found to be 1.06dB:

5.3. Summary of Evaluation Results

Band	Frequency	Highest Output Power (dBm)	Highest Output Power (mW)	Antenna Gain(dBi)	Numeric antenna gain	Power density at 20cm	Limit mW/cm ²
BT 4.2	2402	9.0	7.94	1.06	1.276	0.002	1.000
BLE	2402	9.0	7.94	1.06	1.276	0.002	1.000
WI-FI2.4G 802.11b	2412	19.5	89.13	1.06	1.276	0.023	1.000
WI-FI2.4G 802.11g	2412	18.0	63.10	1.06	1.276	0.016	1.000
WI-FI2.4G 802.11n	2412	18.0	63.10	1.06	1.276	0.016	1.000

The product is under the MPE limits. All is pass.

This antenna gain does approximately correspond with analyses of the radiation pattern produced by these 2 antennas (https://muehlhaus.com/support/antenna/esp32-dual-antenna-simulation):

Antenna 1:

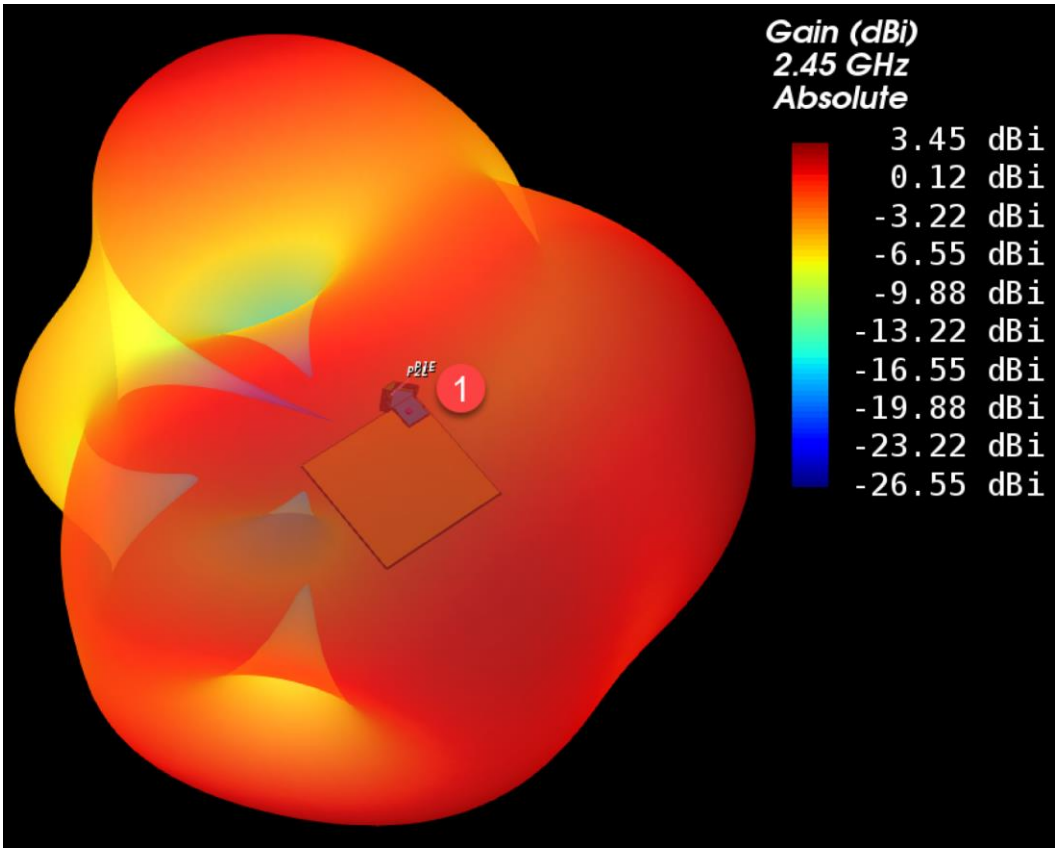

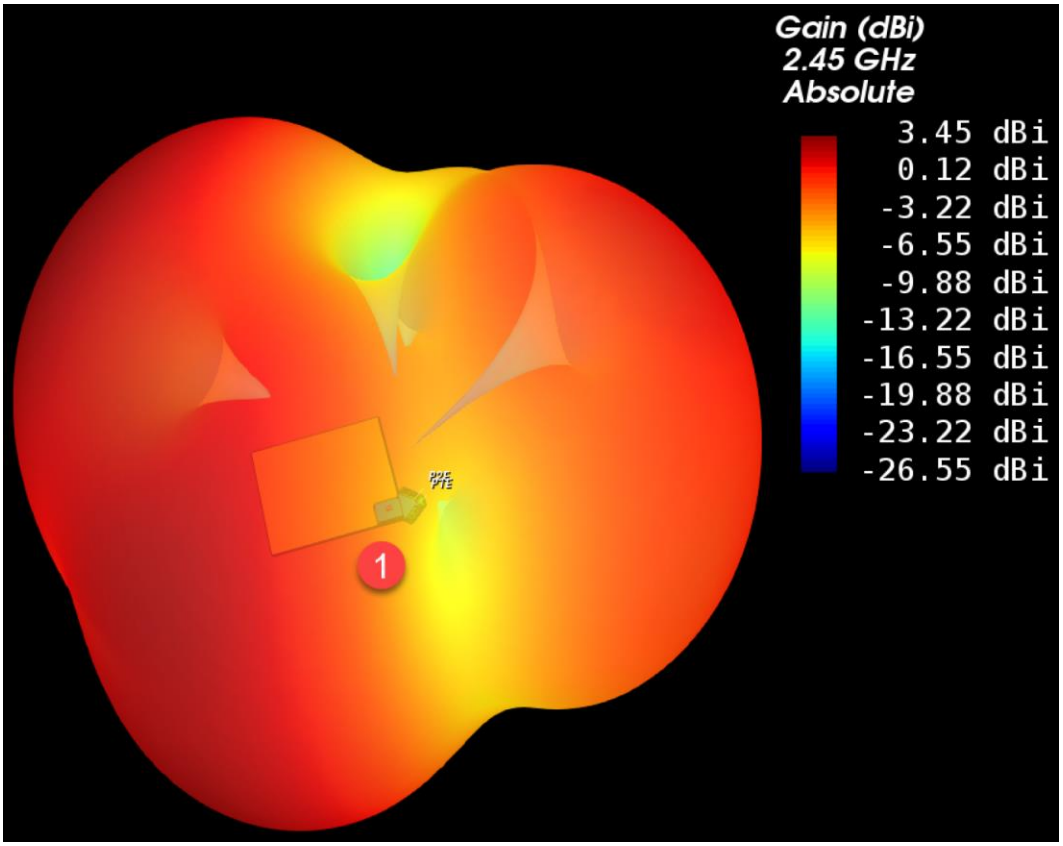
Gain (dBi)
2.45 GHz
Absolute
3.45 dBi
0.12 dBi
-3.22 dBi
-6.55 dBi
-9.88 dBi
-13.22 dBi
-16.55 dBi
-19.88 dBi
-23.22 dBi
-26.55 dBi
1

Antenna 2:

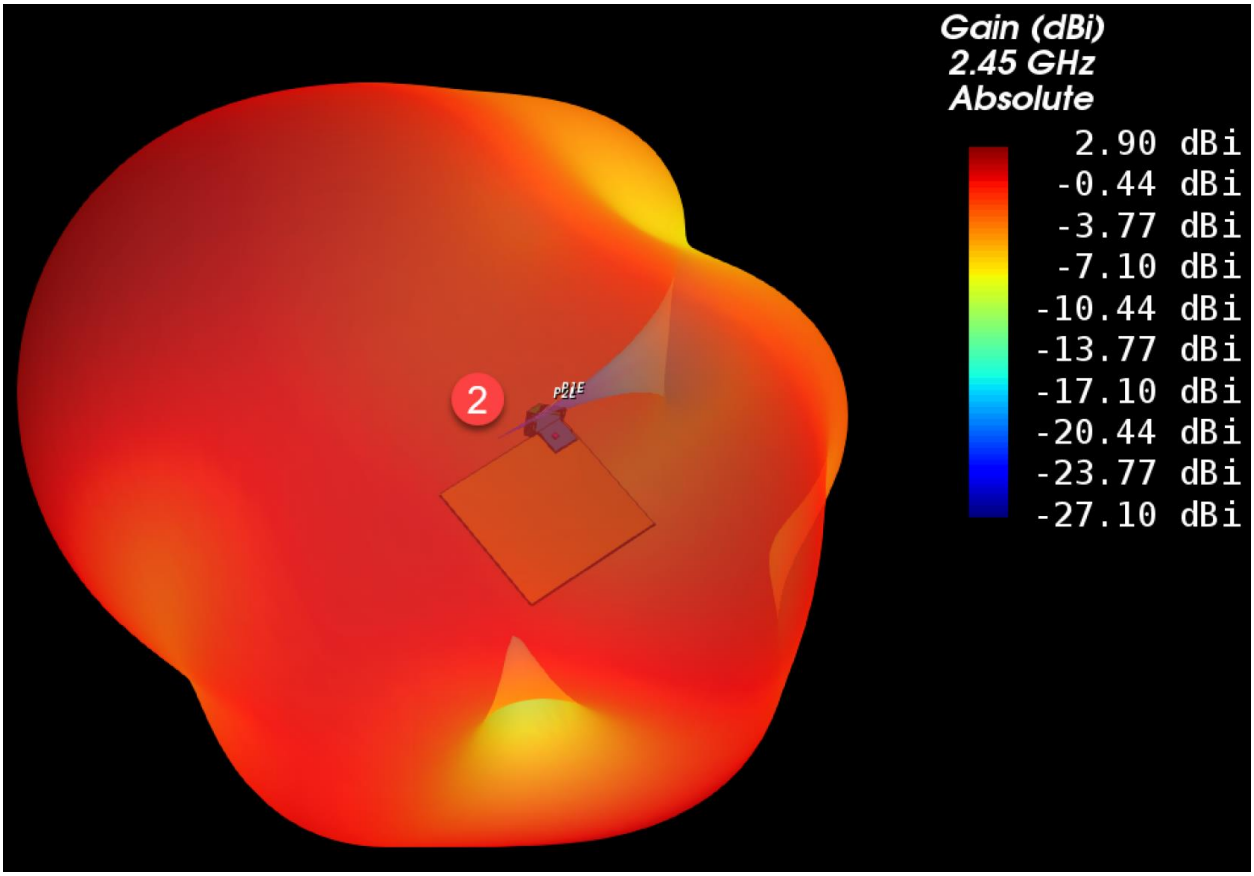
Gain (dBi)
2.45 GHz
Absolute
2.90 dBi
-0.44 dBi
-3.77 dBi
-7.10 dBi
-10.44 dBi
-13.77 dBi
-17.10 dBi
-20.44 dBi
-23.77 dBi
-27.10 dBi
2

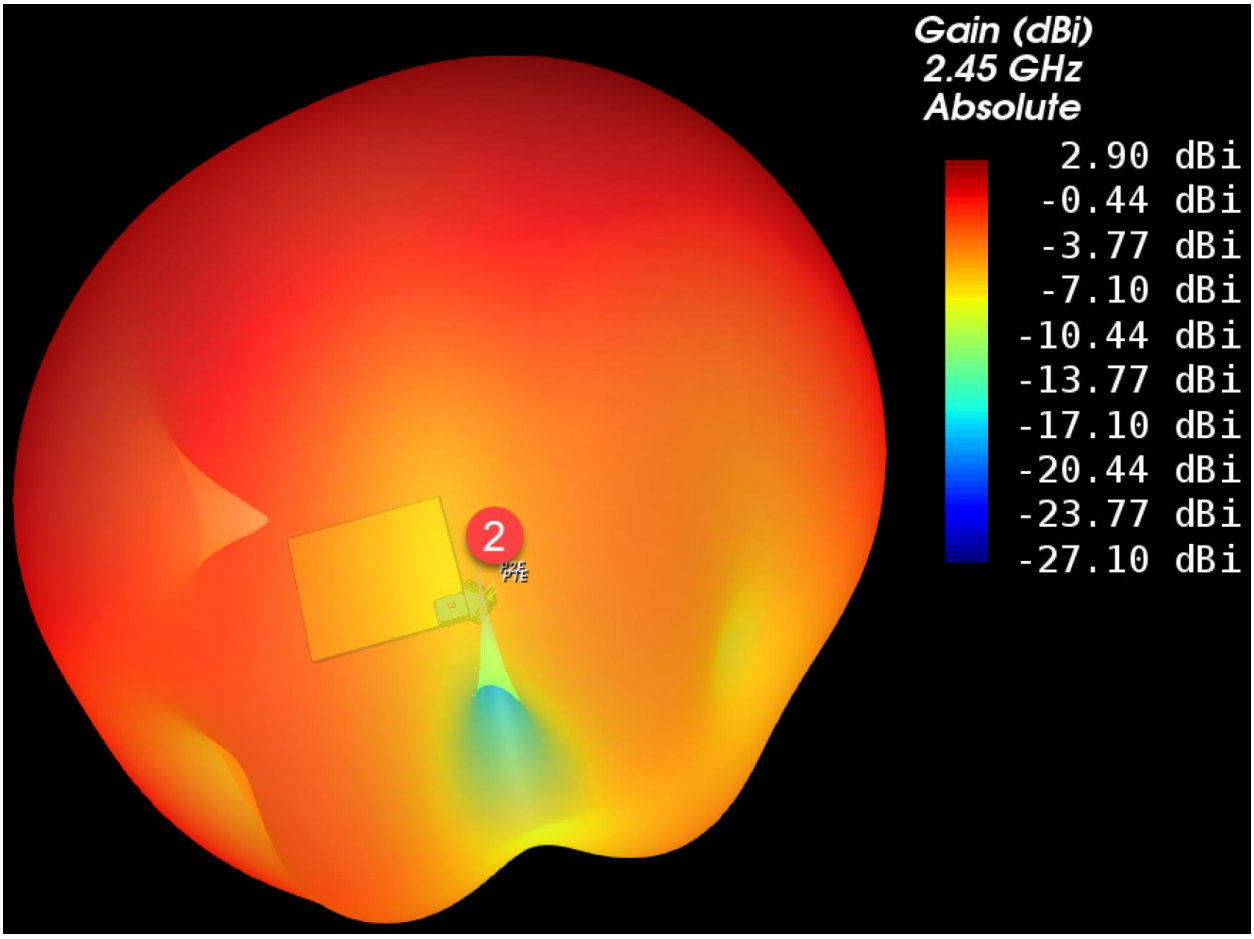

Polar antenna pattern in the PCB plane:

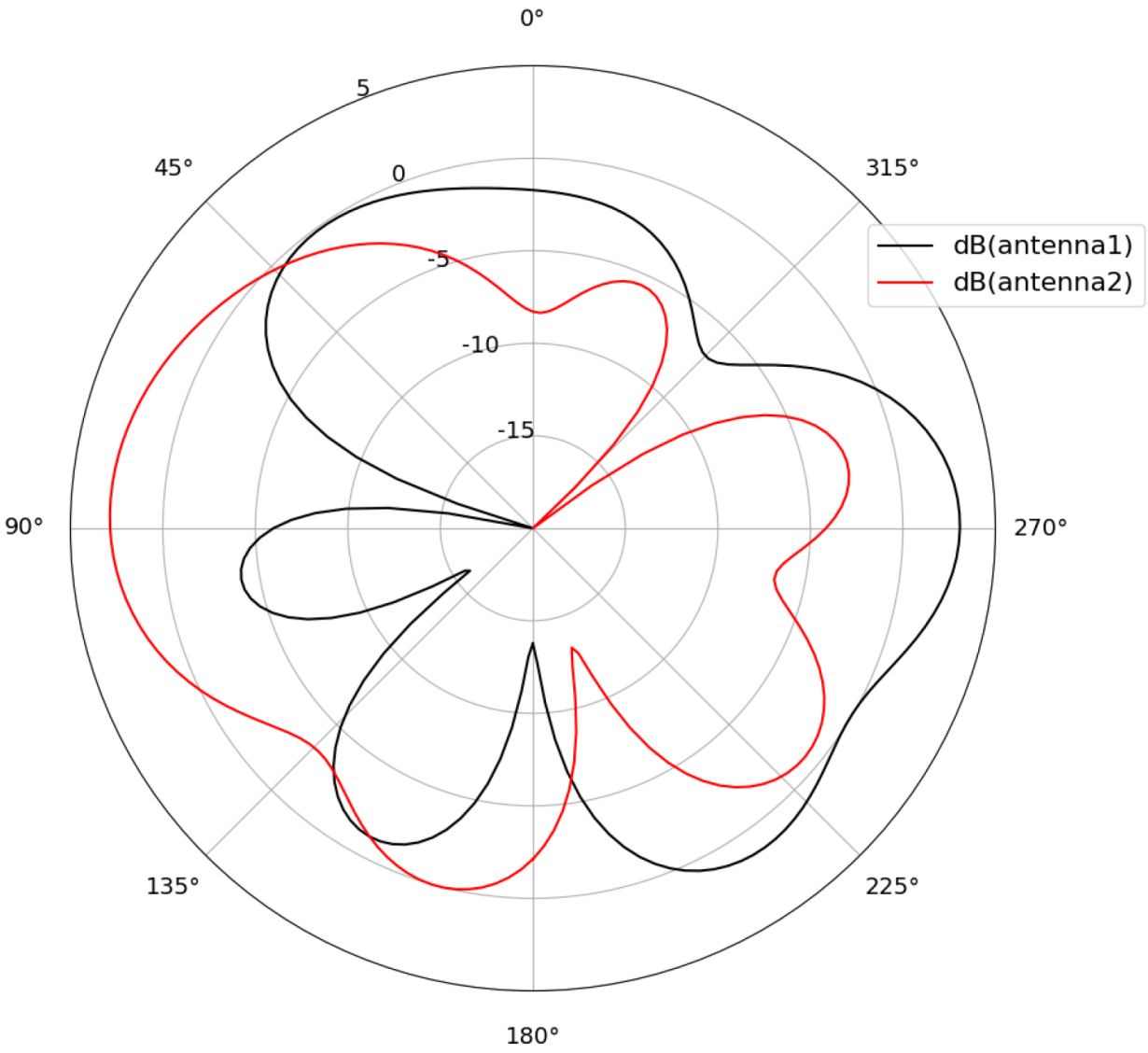
0°
45°
315°
90°
270°
135°
225°
180°
5
0
-5
-10
-15
dB(antenna1)
dB(antenna2)

Application Report

mmWave Radar Radome Design Guide

Chethan Kumar, Habeeb Ur Rahman Mohammed and Greg Peake

ABSTRACT

Radar technology has evolved in last decades from military applications such as missile control, ground surveillance, air traffic control to numerous automotive and industrial applications such as adaptive cruise control, park assist, autonomous parking, motion and presence detection, level sensing, people counting and more. In order for a radar sensor to perform flawlessly in these applications it is critical to ensure that the radome or housing is designed to minimize electrical and environmental interferences to the radar sensor antenna. This application report provides an introduction to radome design and highlights key care abouts for designing a mmWave radome whilst considering the radar sensor performance. It describes a concept of radome design considerations, along with radome test and qualification. Examples of different radome structures are presented with supporting design simulations and measurement results.

Table of Contents

List of Figures

Trademarks

List of Tables

Trademarks

Teflon® is a registered trademark of Teflon.

All trademarks are the property of their respective owners.

1 Introduction and Challenges

A radome (radar dome) is an electromagnetically transparent protective shield that encloses mmWave Radar sensors and the antenna. It protects the mmWave antenna and electronics from external environment effects such as rain, sunlight, wind providing structural weatherproof enclosure. The radome minimally attenuates the electromagnetic signal transmitted or received by the antenna and as such should effectively be transparent to radio waves.

In some cases, a radome could be constructed as a lens that alters the beam characteristics intentionally. Such a radome or lens needs to be designed using electro-magnetic simulation tools in conjunction with the antenna and desired field of view in consideration.

Based on the needs of specific end equipment, radomes can be constructed in several shapes such as planar, spherical, and geodesic where the shape will have some influence on the radiation pattern or field of view and maximum achievable distance by radar sensor. The radome material choice, such as fiberglass, PTFE-coated fabric, and polycarbonate, is generally dependent on the targeted application environmental use.

2 Radome Design Elements

2.1 Understanding Dielectric Constant and Loss tangent on Radome and Antenna Design

In order to understand the electromagnetic wave propagation in a material it is important to know the material constitutive parameters, such as, permittivity, permeability and conductivity. These constitutive parameters characterize the EM properties of the material. From these parameters, special care must be taken in selecting the radome material with optimum relative permittivity (E_r) or dielectric constant (Dk). (Most radomes are designed out of a non-magnetic dielectric material such that the relative permeability = 1 and the conductivity = 0.) Signal fade or “loss” occurs either by the reflection of the electromagnetic waves at the boundary of radome structure or due to multiple reflections within the radome material itself. This is mainly due to the difference in dielectric constant (Dk) of the radome relative to air. The dielectric constant (Dk) represents the reflective, as well as the refractive, properties of a material. In general, the electromagnetic signal can be thought of as “slowing down” as it moves through the radome when compared with air.

Definition of loss tangent: Dielectric loss quantifies a dielectric material's inherent dissipation of electromagnetic energy. It can be parametrized in terms of either the loss angle δ or the corresponding loss tangent tan δ.

The dielectric constant and loss tangent together specify the transmission efficiency of a radome combined with an antenna system where both together are ideally measured at the intended operating frequencies. Dielectric loss quantifies a dielectric material's inherent dissipation of electromagnetic energy. It can be parametrized in terms of either the loss angle δ or the corresponding loss tangent tan(δ). The lower the dielectric constant and loss tangent, the smaller the effect of the radome on the antenna performance. Ideally Dk should be close to 1, since free space Dk is 1. However, it is impractical to use materials that have Dk=1 (basically Styrofoam) since they are not suitable for other goals of the radome (aesthetics, cost, and environmental robustness). Just to note that it is not the antenna design that forces Dk>1, but rather the radome material properties and availability.

2.2 Impedance Mismatch at Radome Boundaries

Electromagnetic wave reflections occur at the boundaries of the plane of mismatch. This plane of mismatch could be considered as boundary of two medium with different dielectric properties, that is, mediums with different permittivity as shown in Figure 2-1.

Figure 2-1. Boundary of Mismatch Between Dielectric Mediums

Radome Design Elements

These reflections due to impedance mismatch can be better understood by looking into electromagnetic wave interaction at the impedance mismatch planes. The interaction of the electromagnetic wave at these planes leads to the reflection and transmission of waves at the boundary of medium, which is quantized in terms of reflection coefficient Γ and transmission coefficient τ. The reflection coefficient is the ratio of reflected E_r and incident E_i electric field strength and transmission coefficient is the ratio of transmitted E_t and incident E_i electric field strength as shown in Equation 1 and Equation 2.

$$\Gamma = \frac{E_r}{E_i} = \frac{\sqrt{\varepsilon_1} - \sqrt{\varepsilon_2}}{\sqrt{\varepsilon_1} + \sqrt{\varepsilon_2}} \tag{1}$$

$$\tau = \frac{E_t}{E_i} = \frac{2 \cdot \sqrt{\varepsilon_1}}{\sqrt{\varepsilon_1} + \sqrt{\varepsilon_2}} \tag{2}$$

Note

(1) and (2) are the reflections at only a single interface boundary.

Essentially, there will be multiple reflections occurring within the radome material and resulting in the accumulation shown in Figure 2-2. This results in a reflected wave (E_{rT}) and transmitted wave (E_{tT}) created from the incident wave (E_{ri}).

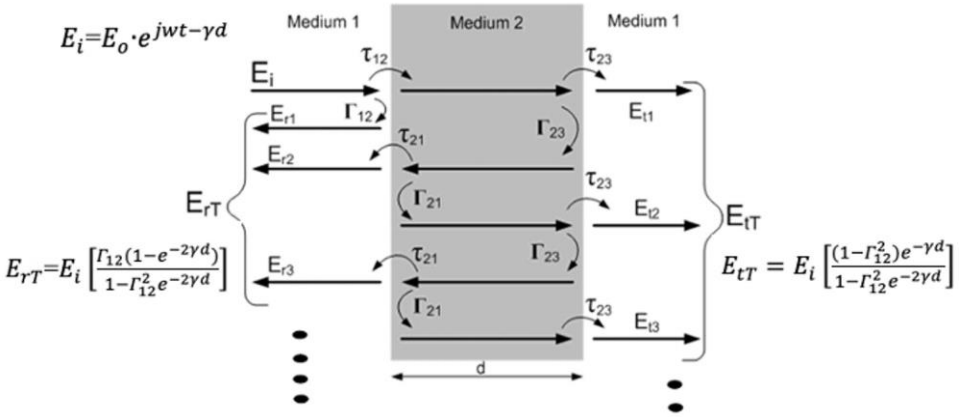

Figure 2-2. Multiple Reflections at Boundaries of Dielectric Mediums

Radome Design Elements

Reflections within the radome can be simplified as shown in Figure 2-3. Free space or air wave impedance is about 377Ω such that the wave impedance inside the radome is given by $377/\sqrt{\varepsilon_r}$ Ω. Electromagnetic waves will be reflected back from such that both the air-radome interface and radome-air interface.

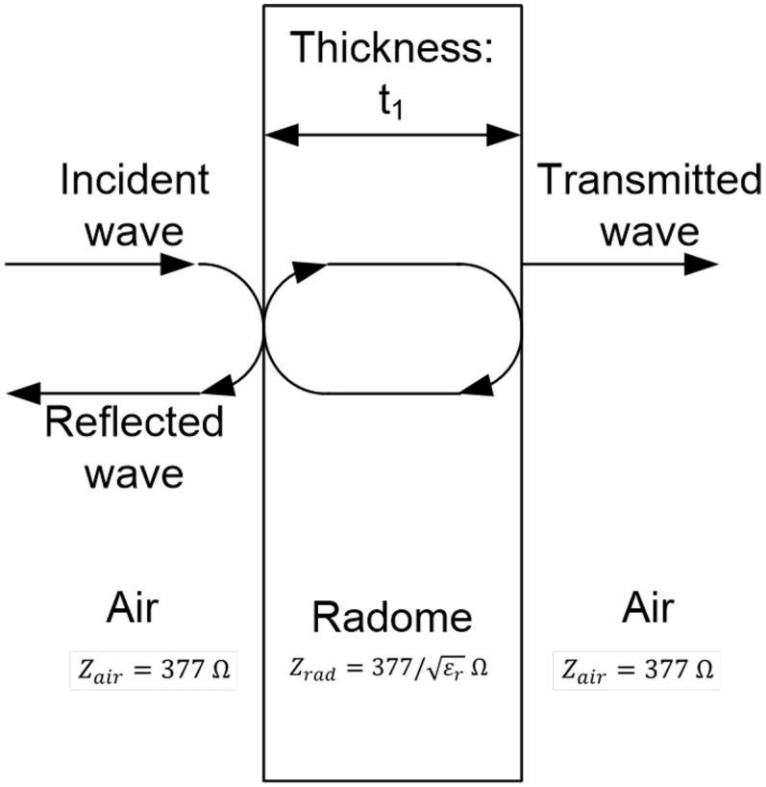

Figure 2-3. Reflections at Radome Boundaries (assumption is that radome has a solid single wall

2.3 Radome Wall Thickness

The wall thickness of the radome plays a key role in arriving at the optimum performance of the mmWave radar sensor. It is important to make sure that the radome wall thickness is equal to an integer multiple of the radar wavelength/2 so that the radome becomes “nearly transparent” for the mmWave frequency range intended. The thickness of radome is given in Equation 3. The wavelength in the radome material becomes shorter versus free air and is an inverse function of the material's dielectric constant as shown in Equation 4.

$$t_{optimum} = \frac{n*\lambda_m}{2} \quad (3)$$

$$\lambda_m = f*C/\sqrt{\varepsilon_r} \quad (4)$$

Where,

- $t_{optimum}$ = Optimum thickness of radome wall or target thickness to make the radome transparent.
- n: 1,2,3…
- λ_m: Wavelength of the material
- C: speed of light

- f: mean carrier frequency used (for example, 62 GHz for a typical 60-64 GHz bandwidth) • ε_r : relative permittivity

Radome Design Elements

In general, radome performance depends mainly on the frequency of use, thickness, ε_r, incident angle, and shape. For the normal incident case, optimum thickness given in Equation 4 is plotted in Figure 2-4 and Figure 2-5.

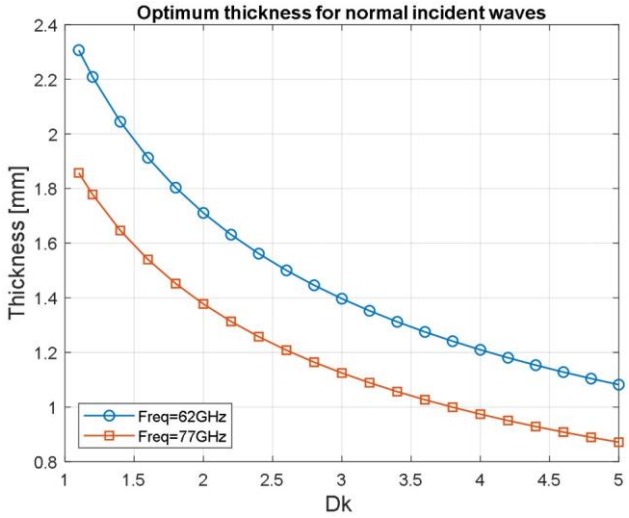

Figure 2-4. Radome Optimal Thickness versus Dielectric for Incident Waves of Different Frequency

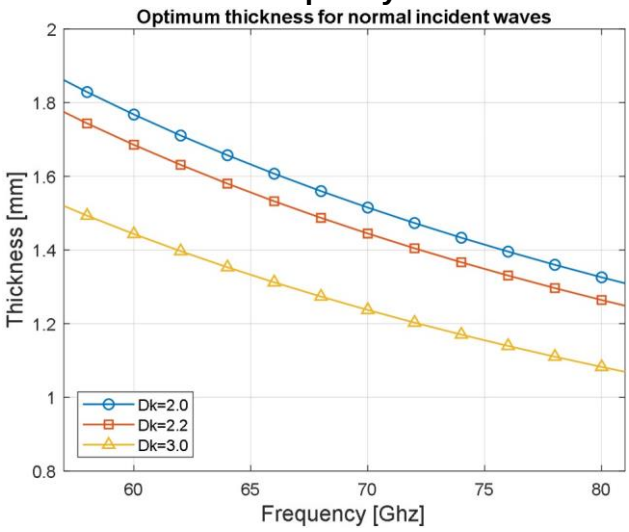

Figure 2-5. Radome Optimal Thickness versus Frequency for Different Dielectrics

2.4 Antenna to Radome Distance

The optimal distance between the antenna and the internal surface of the radome helps to minimize the effects of reflections caused by the radome. These effects become minimal if the waves returned to the antenna are in phase with the transmitted waves. Equation 5 shows the optimal distance that should be between antenna and radome

$$\frac{n*\lambda 0}{}$$

$$D = 2 \tag{5}$$

Where,

- n: 1,2,3…
- D: optimal distance between radome and Antenna
- λ_0: wavelength in air

3 Typical Radome Material Examples

Materials with lower Dk (dielectric constant) and Df (loss tangent) are recommended for radome designs. Typical materials used in radomes are PBT (Polybutylene terephthalate), Plexiglas, Polycarbonate, Teflon® (PTFE), Polystyrene, and ABS. It is important to avoid metal fixings and coatings (especially metallic paint that will reduce the signal strength significantly), see [10].

In addition, the material used should be homogeneous in nature, in order to not create any additional Dk boundaries within the radome itself, with the design aiming for the walls to be solid with no air bubbles or other material fragments inside. There are radome designs that incorporate a sandwich structure with different materials, mainly for strength and possible bandwidth improvements, but those types are not covered in this document.

Table 3-1. Permittivity and Dissipation Factor for Different Radome Materials

Materials	Permittivity (εr)	Dissipation Factor (tanδ)
Polycarbonate	2.9	0.012
ABS	2.0-3.5	0.0050-0.019
PEEK	3.2	0.0048
PTFE (Teflon®)	2	<0.0002
Plexiglass®	2.6	0.009
Glass	5.75	0.003
Ceramics	9.8	0.0005
PE	2.3	0.0003
PBT	2.9-4.0	0.002

4 Radome Angle Dependent Error

Depending on type of radome, the distance traveled in the radome material can be angle dependent. For a rectangular radome distance, the traversed radome wall would be larger at higher grazing angles. In a curved radome, both at boresight and at the higher grazing angles, the distance traveled through the radome is the same; therefore, the angle dependent error would be lower.

4.1 Rectangular Radome Angle Dependent Error

Electrical distance traveled through the radome in boresight is equivalent to the thickness of the radome wall. However, this distance increases as angle of arrival increases and results in a higher angle estimation error. This effect is shown in Figure 4-1.

The theory behind this phenomenon is such that if the radome wall thickness is designed to be λ/2 (half wavelength), then the round trip of the radar signal passing through the inner wall surface, then reflected back from the outer wall surface introduces a net 180° phase shift (180° -180° + 180°) emitted from the inner wall.

Therefore, at boresight of the rectangular radome, the reflections at the inner wall will cancel since they are out of phase, resulting in low net reflections. However, when moving away from the boresight to higher grazing angles of arrival, the distance traveled by the mmWave signal is greater than “optimal thickness” or “half-wavelength”. This causes multiple reflections at the radome interface boundary resulting in ripples in the antenna radiation patterns and leading to nulls. These ripples and nulls can cause inconsistency in the detection of the objects at higher grazing angles resulting in angle estimation errors. This effect can be counteracted by tapering the radome wall towards the extents of the radar FoV, however, this will also compromise the strength of the radome.

Radome Angle Dependent Error

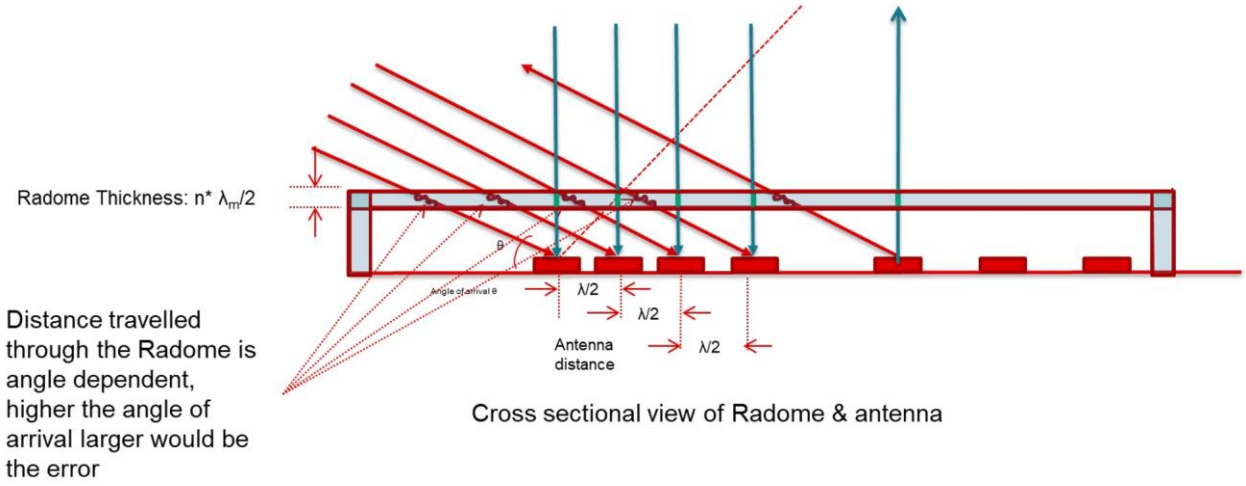

Figure 4-1. Distance Traveled in Rectangular Radome Wall for Different Grazing Angles

4.2 Spherical Radome Angle Dependent Error

Figure 4-2 shows the distance traveled through a curved shaped spherical radome. In this case, at different grazing angles, the radome performance can be shown to be similar to the boresight.

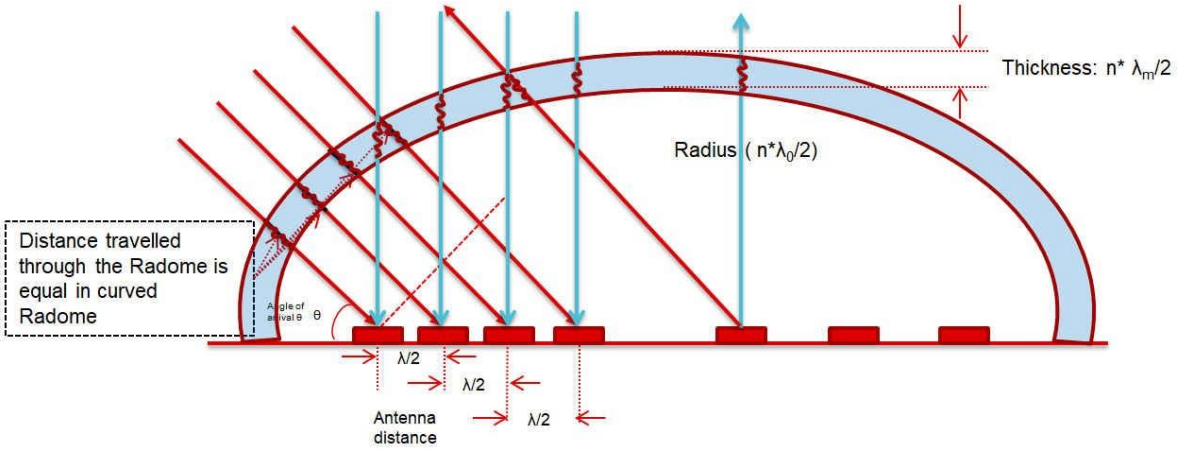

Figure 4-2. Distance Traveled in Spherical Radome Wall for Different Grazing Angles

Radome Angle Dependent Error

4.3 Effect of the Angle Error in the Application

Figure 4-3 and Figure 4-4 shows the effect of the angle estimation error on the detected objects due to both rectangular and spherical radome. Due to the larger distance traveled at higher grazing angles in rectangular radomes, the latter is more prone to an angle estimation error relative to spherical radome structures. It may appear that the object is displaced from the original location. This angle estimation error gets more severe as object to radar distance increases.

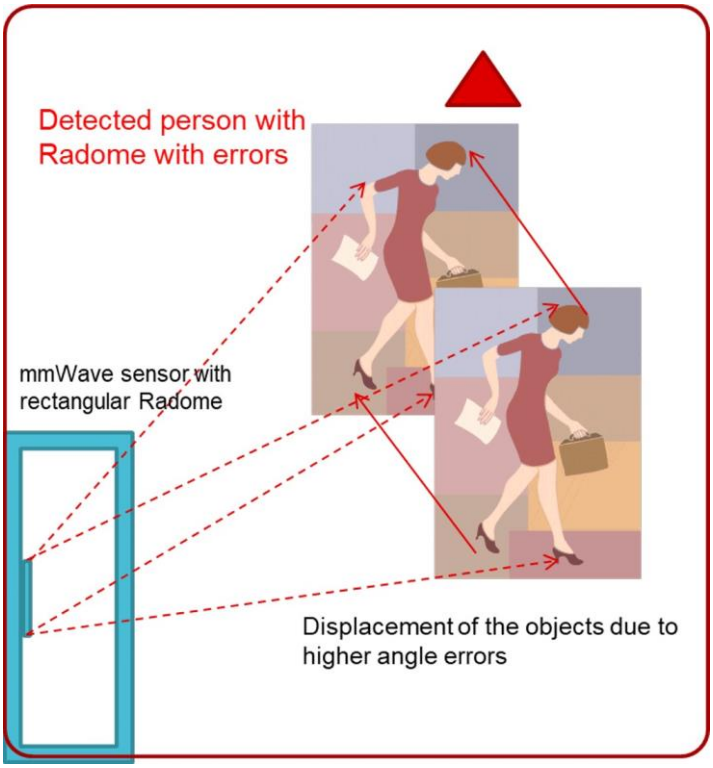

Figure 4-3. The Effect of Angle Estimation Error With Rectangular Radomes

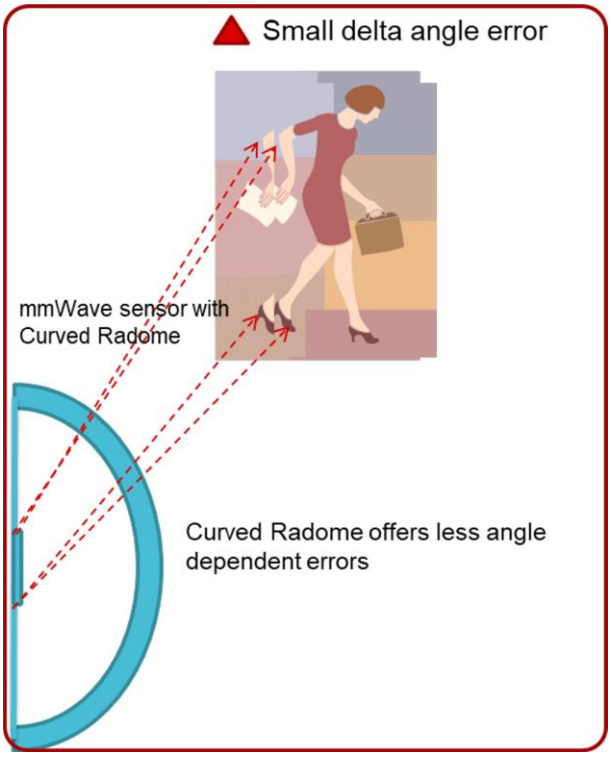

Figure 4-4. The Effect of Angle Estimation Error With Spherical Radomes

5

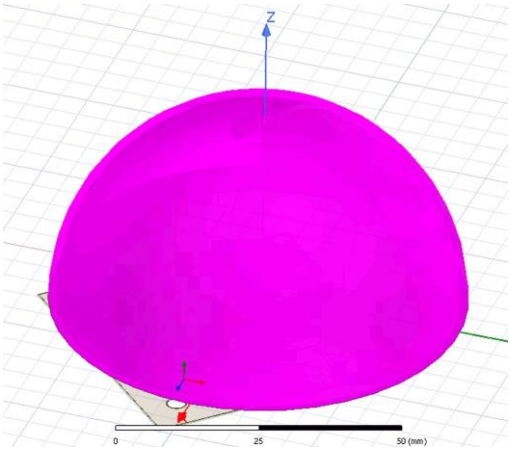

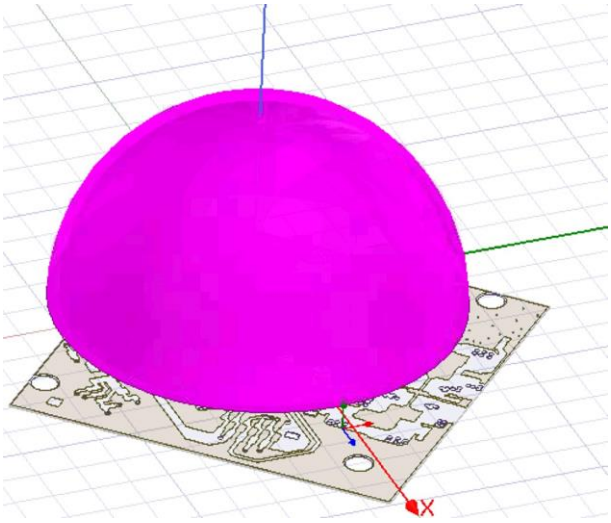

Radome Design and Simulations

This section highlights some radome designs and simulations performed with the IWR6843 ISK style antenna using a spherical radome as a case study. In this section, far-field antenna radiation patterns with and without radome are compared. For this simulation, a derivative of the IWR6843 ISK EVM design is being used.

Figure 5-1 through Figure 5-4 show the pictures of the radome simulations in a 3D EM field solver tool such as the HFSS from Ansys.

Figure 5-1. Spherical Radome HFSS Model: 37.44 mm outer radius

Figure 5-2. Spherical Radome HFSS Model: 18.24 mm Outer Radius

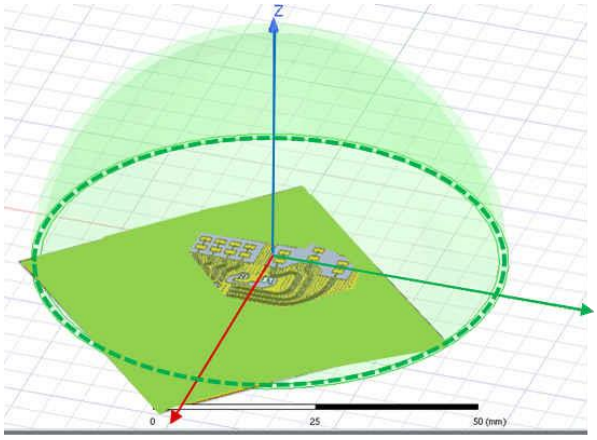

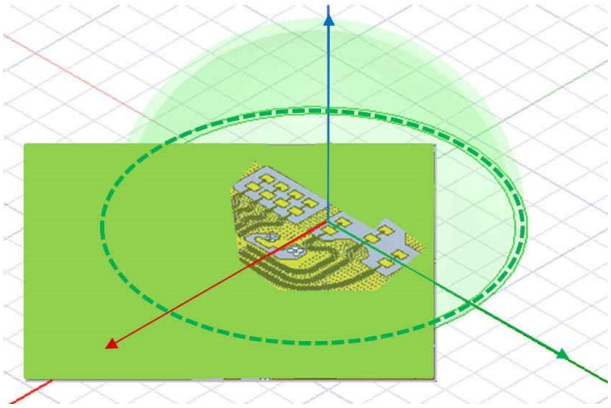

Figure 5-3. Smaller Spherical HFSS Model: Corresponding Dimensions and Placement With Semi-Transparent View of PCB

Figure 5-4. Larger Spherical HFSS Model: Corresponding Dimensions and Placement With Semi-Transparent View of PCB

Figure 5-5 shows the spherical radome design with radius selected based on the antenna aperture size and desired field of view requirements. In this case, the design is optimized for a ±70 degree Azimuth and ±40° elevation field of view. The radius of curvature selected is optimized for an integer multiple of $\lambda_0/2$. For analysis purposes, ABS-HG_FR material is used with Dk of 2.8 and Df of 7.90E-03.

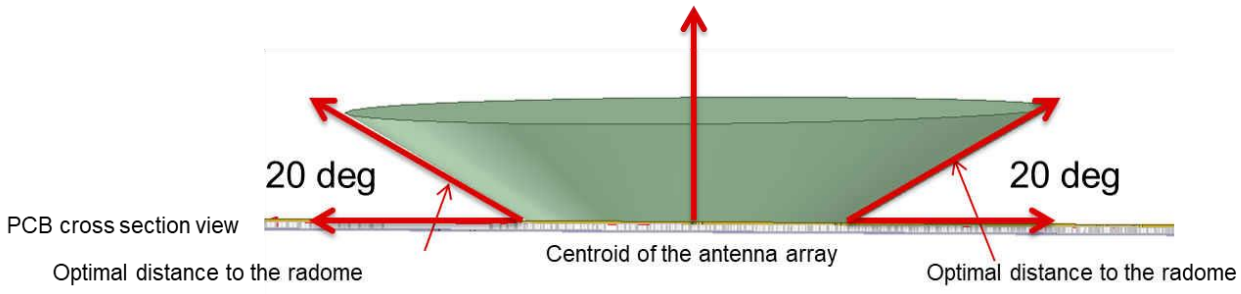

Figure 5-5. Radome Radius of Curvature is Based on Antenna Aperture and FoV Requirement

The following images show simulated antenna radiation patterns for various outer radius integer multiples of $\lambda_0/2$ (18.24 mm, 31.2 mm, 37.44 mm) with the optimal thickness in comparison to the no radome pattern. For the TX images, the three transmitters of the IWR6843 are shown, and similarly for the RX images, the four receivers are shown in different colors. Both the azimuth and elevation aspects are analyzed in the comparison. Based on the ripples seen in the antenna patterns and antenna gains at the edge of the FoV, the 31.2 mm radius seems to be optimal for this design. Approximately 2-3 dB of two-way loss could be expected and needs to be accounted for in the system link budget analysis.

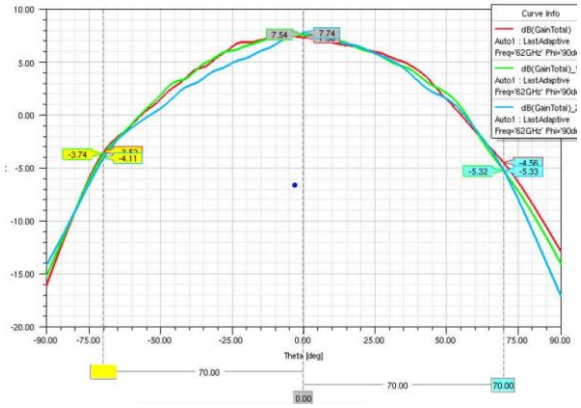

Figure 5-6. Radiation Pattern Tx. Azimuth Without Radome

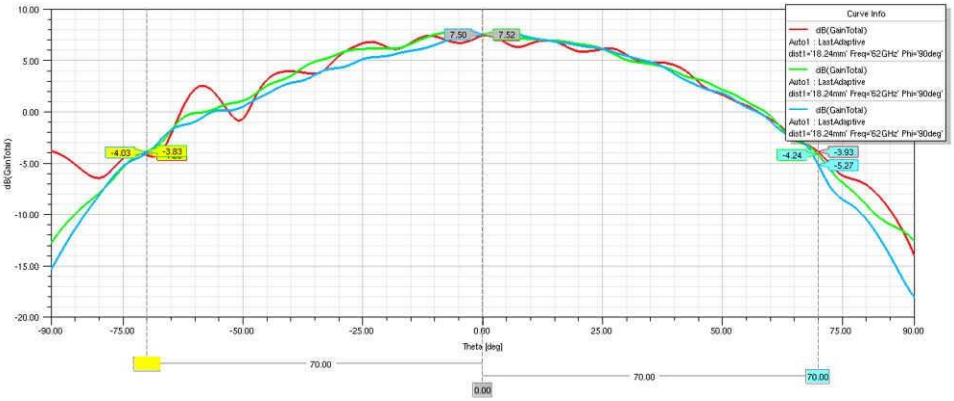

Figure 5-7. Radiation Pattern Tx Azimuth With Radome Radius 18.24 mm

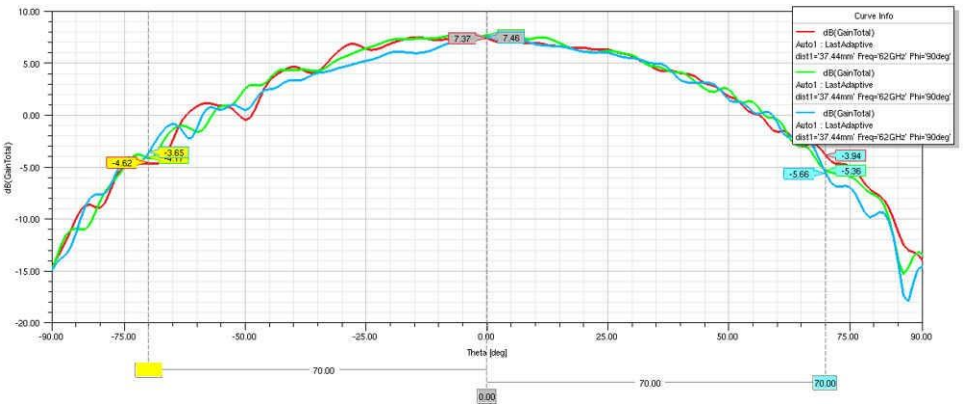

Figure 5-8. Radiation Pattern Tx Azimuth With Radome Radius 37.44 mm

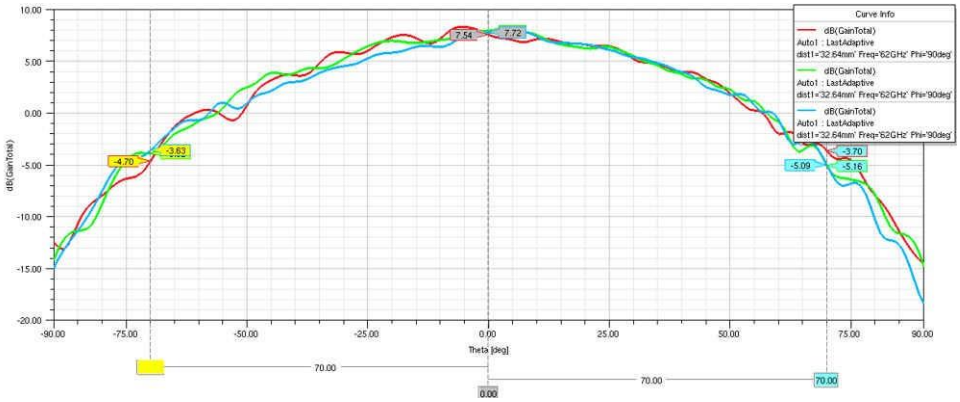

Figure 5-9. Radiation Pattern Tx Azimuth With Radome Radius 32.64 mm

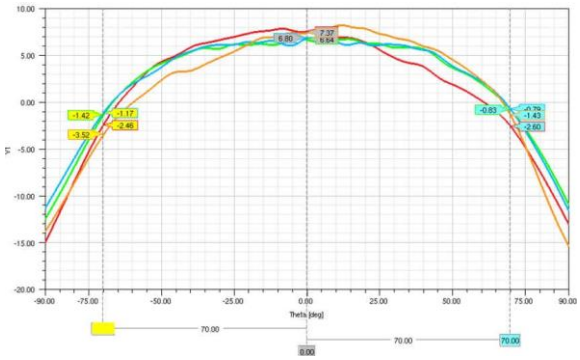

Figure 5-10. Radiation Pattern Rx Azimuth Without Radome

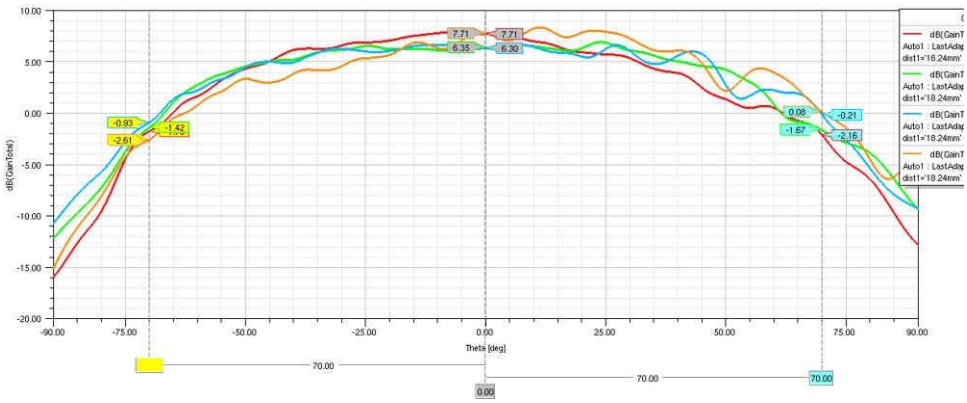

Figure 5-11. Radiation Pattern Rx Azimuth With Radome Radius 18.24 mm

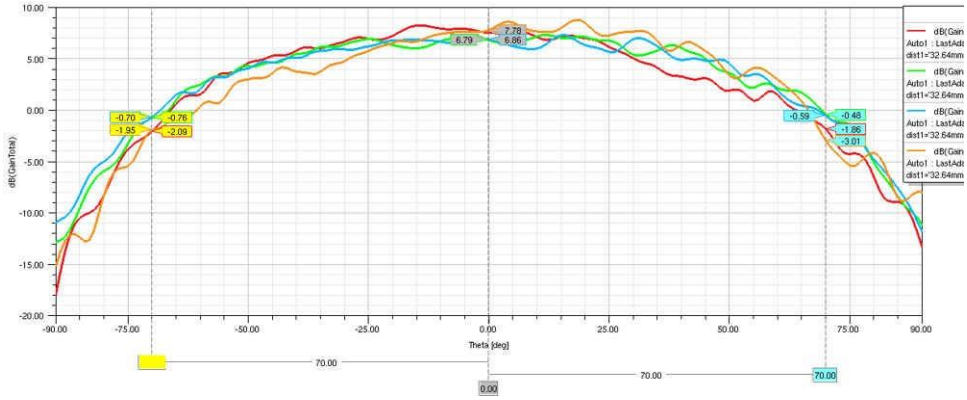

Figure 5-12. Radiation Pattern Rx Azimuth With Radome Radius 37.44 mm

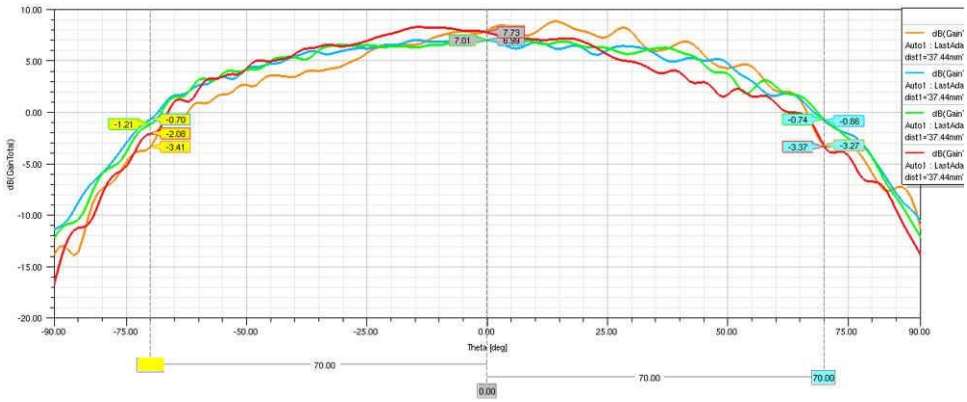

Figure 5-13. Radiation Pattern Rx Azimuth With Radome Radius 32.64 mm The following images show a similar analysis is done for the elevation field of view. For the ±40° elevation field of view, there is minimal ripple impact seen due to radome.

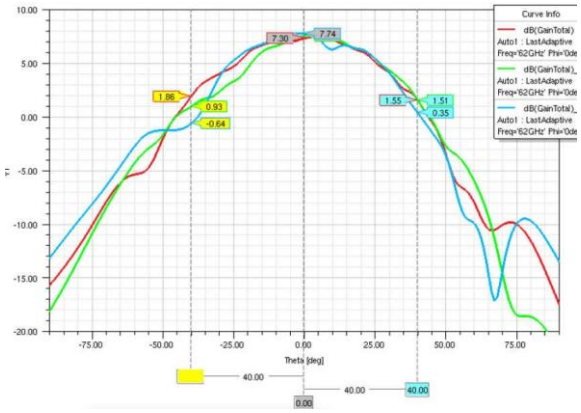

Figure 5-14. Radiation Pattern Tx. Elevation Without Radome

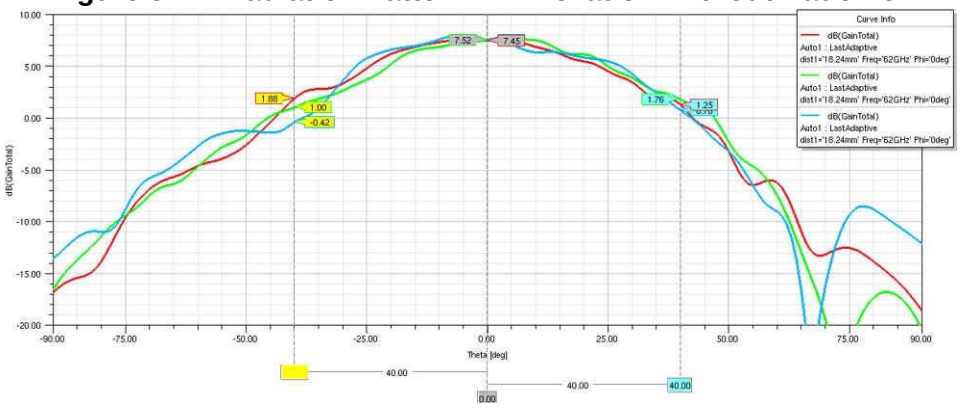

Figure 5-15. Radiation Pattern Tx Elevation With Radome Radius 18.24 mm

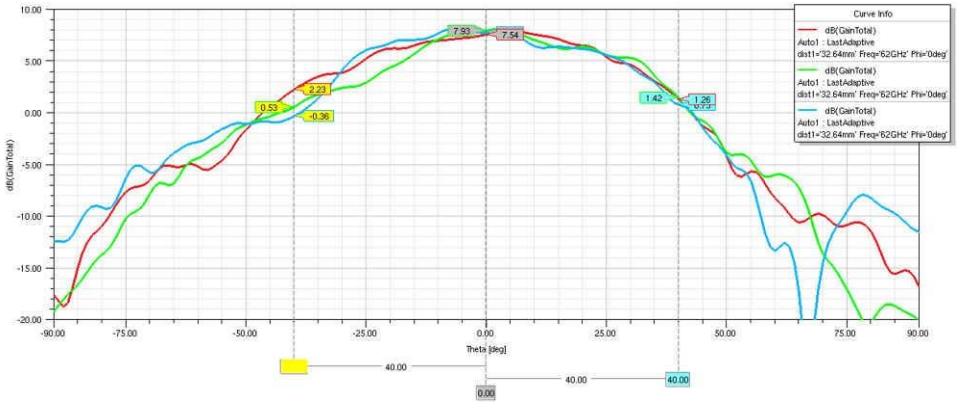

Figure 5-16. Radiation Pattern Tx Elevation With Radome Radius 37.44 mm

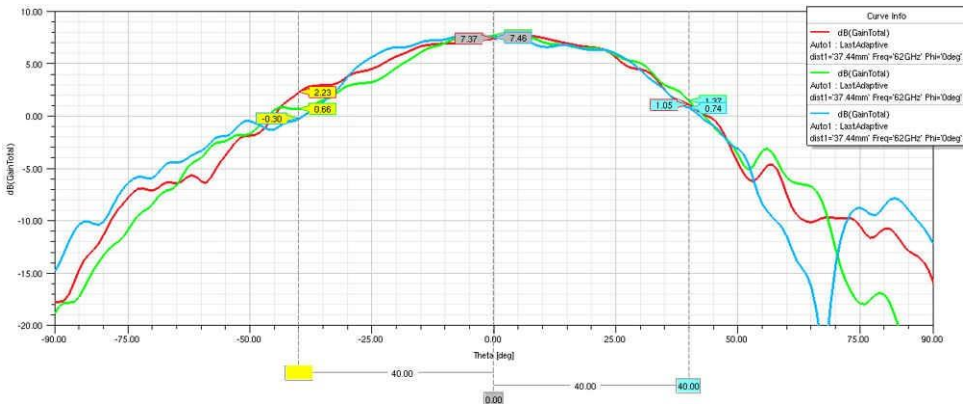

Figure 5-17. Radiation Pattern Tx Elevation With Radome Radius 32.64 mm

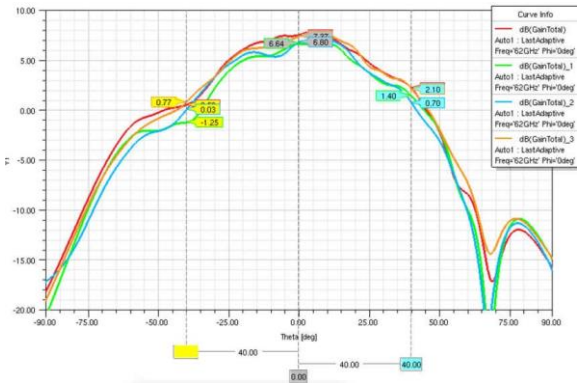

Figure 5-18. Radiation Pattern Rx Elevation Without Radome

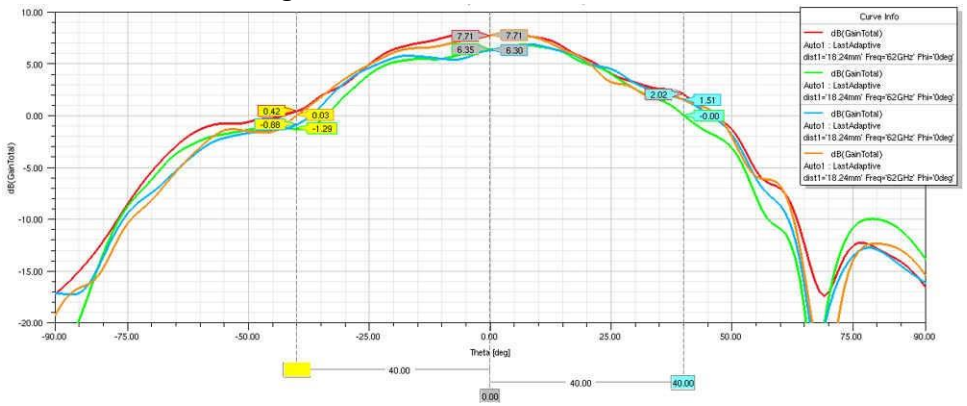

Figure 5-19. Radiation Pattern Rx Elevation With Radome Radius 18.24 mm

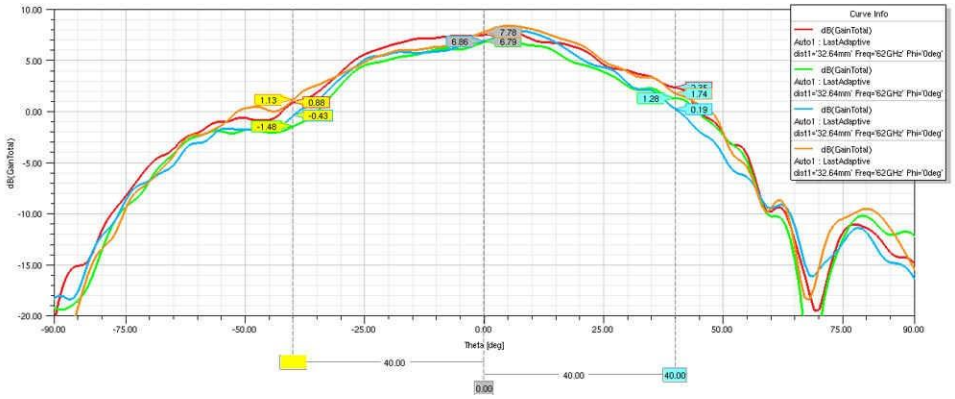

Figure 5-20. Radiation Pattern Rx Elevation With Radome Radius 37.44 mm

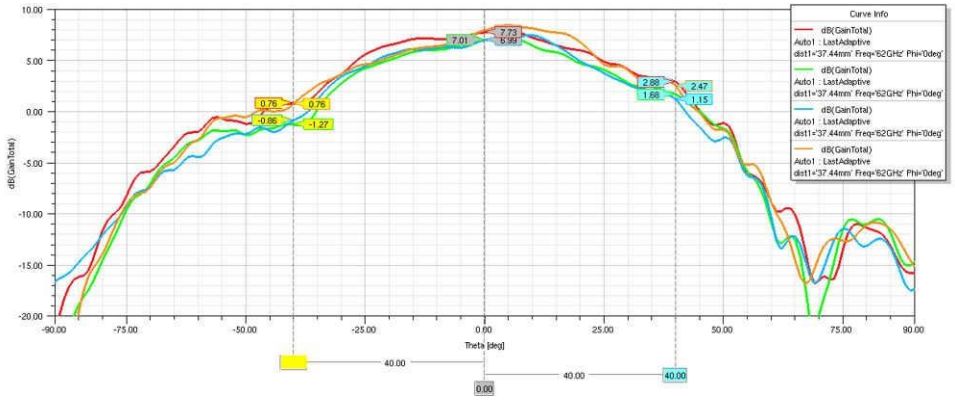

Figure 5-21. Radiation Pattern Rx Elevation With Radome Radius 32.64 mm

6 Radome Lab Experiments

Lab measurements have been done using multiple radomes of different material, shape and thickness. This section provides the measurement results for the different radomes.

6.1 Radome Experiment – 1: Flat Plastic Radome

A radome with 2 mm thickness is chosen with ABS plastic material construction. Figure 6-1 shows the picture of this radome. Experiments are conducted centered around 62 GHz frequency on an IWR6843ISK EVM board.

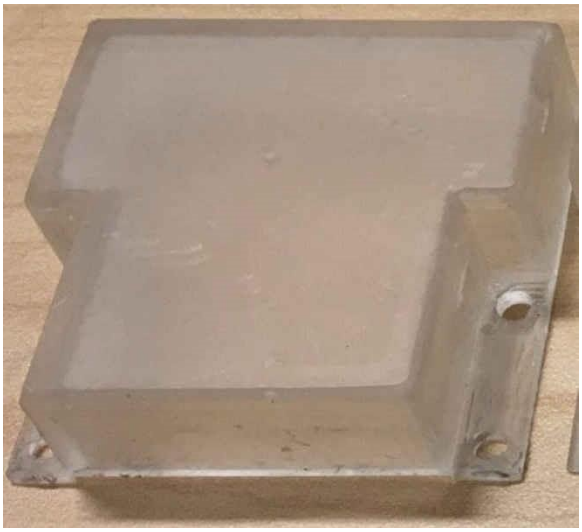

Figure 6-1. ABS Plastic Rectangular Radome With 2 mm Wall Thickness

Radome Lab Experiments

Figure 6-2 shows two graphs with the ABS plastic rectangular radome. Figure 6-3 shows antenna radiation pattern without the radome and, correspondingly, Figure 6-2 shows antenna radiation patterns with the radome. It can be seen from the plots that this radome significantly degraded the antenna radiation pattern.

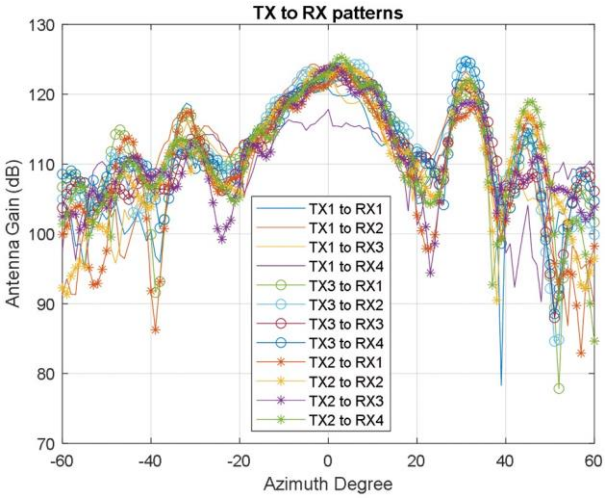

Figure 6-2. Azimuth Antenna Radiation Patterns for the 2 mm Wall Thickness ABS Plastic Rectangular Radome

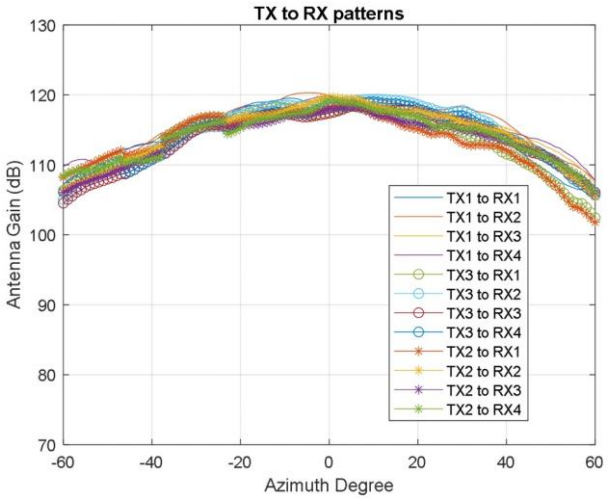

Figure 6-3. Azimuth Antenna Radiation Pattern With no Radome

6.2 PTFE Material Rectangular Radome

In the second experiment a rectangular radome with 1.524 mm wall thickness is chosen with the PTFE sheet material. Figure 6-4 shows the picture of this Radome.

Figure 6-4. PTFE-Based Rectangular Radome With 1.524 mm Wall Thickness

Radome Lab Experiments

Figure 6-5 and Figure 6-6 shows antenna radiation patterns with and without PTFE rectangular radome. It can be seen that using PTFE material reduces the amount of distortion or ripple amplitude compared to the regular

ABS radome. In this case, distortion is less because the radome thickness and material were chosen to optimize transparency across the field of view.

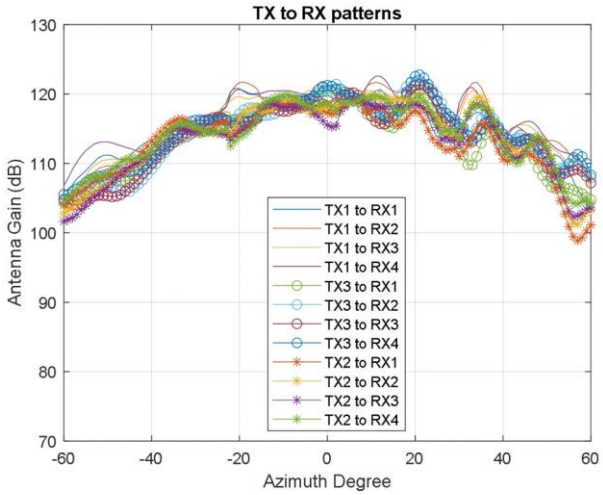

Figure 6-5. Antenna Radiation Measurement With PTFE Rectangular Radome

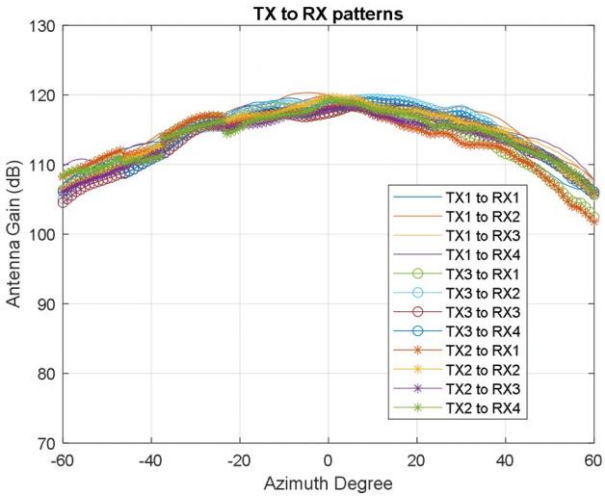

Figure 6-6. Antenna Radiation Measurement With no Radome

6.3 PTFE-Based Curved Radome

The third experiment was performed using a curved shaped radome with 1.524 mm wall thickness using PTFE material as shown in Figure 6-7.

Figure 6-7. The PTFE Curved Shaped Radome With 1.524 mm Wall Thickness

Additional Considerations

Figure 6-8 through Figure 6-11 show the curved shaped PTFE material radome antenna radiation pattern and angle estimation. Compared to rectangular radome, the curved shaped radome shows better results with less distortion or ripples in antenna radiation patterns and lower angle estimation errors at wider FoV angles. The

phase calibration applied in Figure 6-9 and Figure 6-11 is discussed in Section 7.1, and as can be seen in the figures, it shifts the angle error curve such that the estimated angle is adjusted to zero at the antenna boresight.

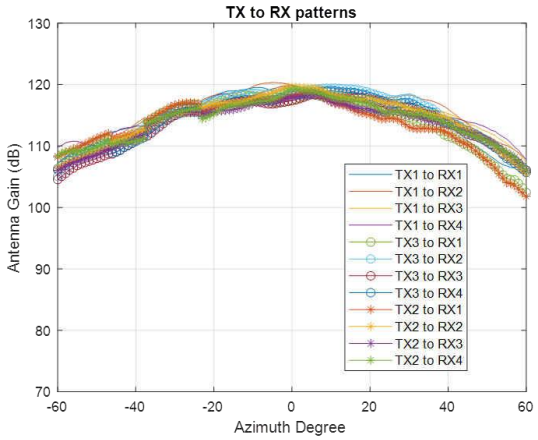

Figure 6-8. Antenna Radiation Pattern Measurement With no Radome

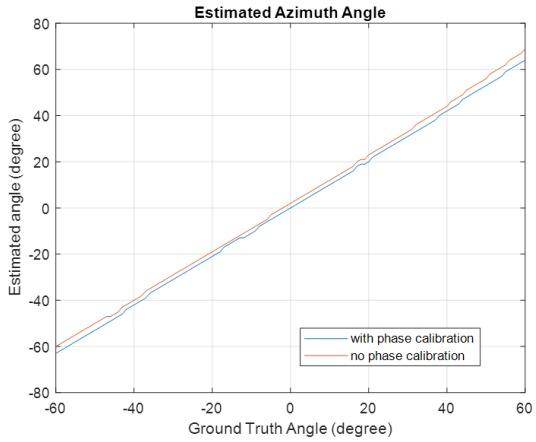

Figure 6-9. Azimuth Angle Estimation Error Measurement With no Radome - With and Without Phase Calibration

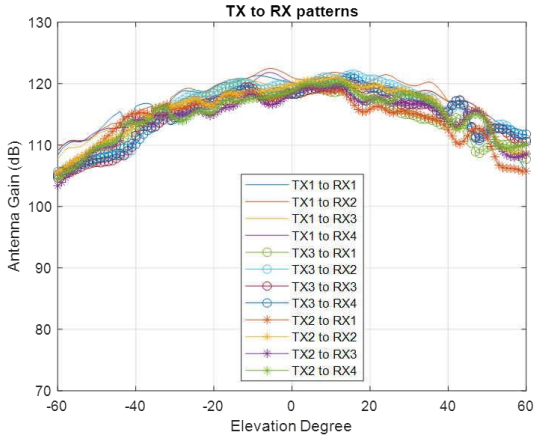

Figure 6-10. Elevation Antenna Radiation Pattern Error With the Curved Shape Radome

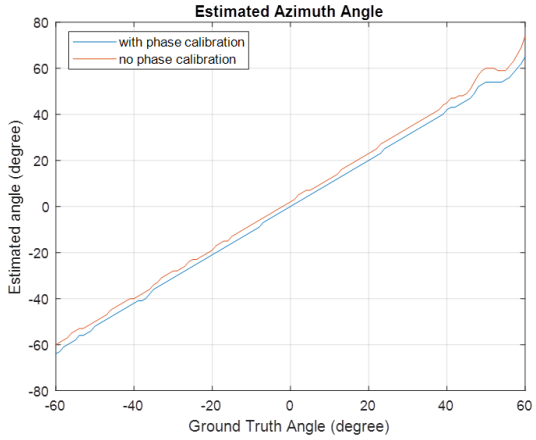

Figure 6-11. Azimuth Angle Estimation Measurement With the Curved Shape Radome - With and Without Phase Calibration

7 Additional Considerations

7.1 Antenna Calibration

To improve antenna performance within a radome, SoC level antenna calibrations can be applied to compensate for bias in the range and receiver gain as well as phase introduced from the RF path delays. At a high level, the goal of this procedure is to determine the range bias offset common to all Tx-Rx paths and the gain and phase mismatch of each virtual Tx-Rx pair of a reference object placed at a fixed known distance in the far field at boresight. For more information on this subject, see [4].

Additional Considerations

The mmWave SDK provides a method for generating the calibration coefficients over the command line interface via the Out of Box (OOB) demo. For more details, see the mmWave SDK User's Guide and look for the compRangeBiasAndRxChanPhase procedure. Additionally, the procedure and implementation of the calibration routine in the data-path processing chain can be found in the mmWave SDK install folder at: mmwave_sdk_<ver>\packages\ti\datapath\dpc\objectdetection\<chain_type>\docs\doxygen\html\index.html . You can use the OOB demo to perform the calibration or port the provided source code into your own custom application.

Additionally, using the same OOB demo application and reading sources, there is a procedure for removing near-field reflection from the air-radome boundaries. There can be antenna coupling signatures in the range bins close to the radar that manifest around DC in the range FFT output (see calibDcRangeSig in the SDK user's guide). The same calibration procedure can also be used to negate any near-field reflections caused by the radome.

7.2 Radome Near Proximity Considerations

The radome will naturally provide an exterior surface where other environmental layers will form, and can subsequently affect the performance of the system. This topic is not discussed in this document, however, some of these example challenges are listed below:

- Wet grass/mud deposits for lawn mowers
- Dust and mud deposits for off road vehicles
- Metallic dust, and other dusts deposits for factory vehicles
- Water absorption of the radome can be an important artifact since the electrical properties will change.
- Ice and snow formation on the radome for cars and outside vehicles or on the exterior of surveillance radar sensors can significantly reduces the dynamic range of the radar detection capability. This is typically handled by embedding a heater into the radome when the radar is deployed in areas where it can be directly exposed to precipitation.

To address some of the above challenges requires either manual or built-in cleaning systems, which can be triggered by the radar system after detecting that RF visibility has been obscured using custom built-in diagnostics.

In the case of an enclosure with metal as part of structure, which can also serve as a heatsink, the metal parts should not protrude into the field of view of antenna.

In some cases, within the radome, to prevent multiple reflections from the radome walls to PCB, it is good practice to use absorber material wherever it's feasible. Other techniques, such as the traditional use of PCB potting for environmental protection, should be avoided when it comes to covering the antenna elements. These materials tend to have a variable thickness with unknown Dk characteristics and can severely degrade the performance of the antenna. However, a very thin (~1 µm) low loss coating material [11] can be used over the antenna structures for if additional protection is required.

8 Summary

The objective of an efficient radome design is to reduce the reflections at its surface for transmission and reception of the signal, with minimum loss and beam distortion. For a general-purpose enclosure that covers the radiating side of the sensor, the material should have a uniform thickness and must also have a good surface smoothness.

Material with lower Dk and Df (dielectric constant and loss tangent) are recommended. Typical materials used in radomes are Polycarbonate, Teflon (PTFE), and Polystyrene. Paint, especially metallic-based, used to enhance the aesthetic appearance of the radome, may further degrade the performance of the antenna. Hence, care needs to be taken while adding paint onto the top surface of radome. Radome and antenna simulations should be performed to determine if there is any degradation in the radiation pattern.

Thin-wall designs have been found to be suitable for use at low microwave frequencies where the wave length of the electromagnetic energy is relatively large. But the resulting walls have had insufficient structural integrity for many microwave applications. A thicker wall design which provides adequate strength and rigidity allows transmission of electromagnetic energy within a relatively narrow bandwidth to which the radome is tuned, however, electrical performance can quickly degrade at frequencies above and below the tuned wall thickness.

Acknowledgments

TI has partnered with companies to offer a wide range of solutions using TI mmWave radar sensors and related services. These companies can accelerate your path to production using mmWave radar. Within this partner network, you will find companies with capabilities of designing both radomes and lens's. To quickly browse our third-party solutions and find the right third-party to meet your needs, use this search tool https://www.ti.com/tool/MMWAVE-3P-SEARCH.

9 Acknowledgments

Authors would like to acknowledge Brian Ginsburg, Eunyoung Seok, Gondalia Akash, Meysam Moallem, Chloe Shay, Anil Kumar KV, and Howard Jiang and team for the contribution to this application report.

10 References

1. Mashury Wahab, Radar Radome and Its Design Considerations, Instrumentation, Communication, Information Technology and Biomedical Engineering (ICICI-BME), 2009 International Conference.
2. Habeeb Ur Rahman Mohammed, Understanding Ripples in RF Performance Measurement, EDN
3. Texas Instruments: *TI mmWave Radar Sensor RF PCB Design, Manufacturing and Validation Guide*
4. Texas Instruments: *mmWave Production Testing Overview*
5. The New Requirements of Plastic Performance for Intelligent Driving of Autocar, PBT Has Great Potential
6. Radome Material supplier:
   - Radome Grades
   - Introducing Materials and Technologies for ADAS Parts - Sensor Edition
7. DK/DF of various material types
   - Dielectric Constant, Strength, & Loss Tangent
8. Reference: Unravelling Polymers 9. Some of the Radome material used:
   - Radome Grades
   - Introducing Materials and Technologies for ADAS Parts - Sensor Edition
   - Electrical Properties of Plastic Materials
   - Electrical Properties of Plastics
10. Reference: Reflection, Refraction, and Self-Jamming
11. Coating/Potting Material Certonal FC-742
12. Near Field and Far Field Regions of an Antenna

13. Joint Antenna-Array Calibration and Direction of Arrival Estimation for Automotive Radars

IMPORTANT NOTICE AND DISCLAIMER

TI PROVIDES TECHNICAL AND RELIABILITY DATA (INCLUDING DATA SHEETS), DESIGN RESOURCES (INCLUDING REFERENCE DESIGNS), APPLICATION OR OTHER DESIGN ADVICE, WEB TOOLS, SAFETY INFORMATION, AND OTHER RESOURCES “AS IS” AND WITH ALL FAULTS, AND DISCLAIMS ALL WARRANTIES, EXPRESS AND IMPLIED, INCLUDING WITHOUT LIMITATION ANY IMPLIED WARRANTIES OF MERCHANTABILITY, FITNESS FOR A PARTICULAR PURPOSE OR NON-INFRINGEMENT OF THIRD PARTY INTELLECTUAL PROPERTY RIGHTS.

These resources are intended for skilled developers designing with TI products. You are solely responsible for (1) selecting the appropriate TI products for your application, (2) designing, validating and testing your application, and (3) ensuring your application meets applicable standards, and any other safety, security, regulatory or other requirements.

These resources are subject to change without notice. TI grants you permission to use these resources only for development of an application that uses the TI products described in the resource. Other reproduction and display of these resources is prohibited. No license is granted to any other TI intellectual property right or to any third party intellectual property right. TI disclaims responsibility for, and you will fully indemnify TI and its representatives against, any claims, damages, costs, losses, and liabilities arising out of your use of these resources.

TI’s products are provided subject to TI’s Terms of Sale or other applicable terms available either on ti.com or provided in conjunction with such TI products. TI’s provision of these resources does not expand or otherwise alter TI’s applicable warranties or warranty disclaimers for TI products.

TI objects to and rejects any additional or different terms you may have proposed.

Mailing Address: Texas Instruments, Post Office Box 655303, Dallas, Texas 75265